

Variation in crustal structure along the Kyushu-Palau Ridge at 15–21°N on the Philippine Sea plate based on seismic refraction profiles

Azusa Nishizawa¹, Kentaro Kaneda¹, Yasutaka Katagiri¹, and Junzo Kasahara²

¹Hydrographic and Oceanographic Department, Japan Coast Guard, Tokyo 104-0045, Japan

²Japan Continental Shelf Survey Co. Ltd., Tokyo 104-0031, Japan

(Received January 6, 2007; Revised May 20, 2007; Accepted May 24, 2007; Online published June 19, 2007)

We acquired coincident wide-angle and multi-channel seismic reflection data along four profiles perpendicular to the Kyushu-Palau Ridge (KPR) between 15°N and 20°N on the Philippine Sea plate. The crustal thickness beneath the KPR, which is a remnant arc created in the Late Eocene, varies along the strike from 8 to approximately 20 km and is always thicker than the adjacent oceanic crust of the West Philippine Basin to the west and the Parece Vela Basin to the east. The thickest crust among the four profiles, which is primarily due to a thickening of the lower crust, is found where the KPR adjoins Oki-no-Tori-Shima Island. There is no clear evidence of the thick (>5 km) middle crustal layer with a *P*-wave velocity of 6.0–6.5 km/s that has been inferred beneath the conjugate rifted counterpart of the Izu-Ogasawara(Bonin)-Mariana Island-arc. Our results suggest that the crust of the KPR at 15–21°N represents a less mature island arc crust relative to that further north along the ridge where a mid-crustal layer of 6 km/s has been reported.

Key words: Kyushu-Palau Ridge, Oki-no-Tori-Shima island, West Philippine Basin, seismic refraction, crustal structure.

1. Introduction

The Kyushu-Palau Ridge (KPR) is a bathymetric high, extending north-south near the center of the Philippine Sea (Fig. 1). It is considered to be a remnant of the proto Izu-Ogasawara (Bonin)-Mariana (IBM) Island arc that was separated when backarc spreading began in the Shikoku and Parece Vela Basins (e.g. Okino *et al.*, 1999). *P*-wave velocity models of the Izu-Ogasawara Island arc have been obtained in the north at 32°15'N by Suyehiro *et al.* (1996) and further south near 30.5°N by Nishizawa *et al.* (2006). Takahashi *et al.* (2007) presented a new velocity model across the Mariana arc at 17°N. The above results suggest that there is no significant along-strike variation in the arc crust of these regions and that the arc is characterized by a middle crust with a *P* velocity of 6.0–6.5 km/s and a thickness of approximately 5 km, a lower crust with a *P* velocity of 6.7–7.3 km/s and a thickness of approximately 8 km, and a total crustal thickness of approximately 20 km. Recent preliminary results of wide-angle seismic profiles along the Izu-Ogasawara arc further south of 30°N have shown significant differences in a thickness and average velocity of the crust along the arc (e.g., Kodaira *et al.*, 2006).

Only a few seismic studies of the KPR region have been conducted, and variations in crustal structure along the KPR are relatively poorly known. A comparison of the tectonically active IBM Island arc with the inactive KPR remnant arc can constrain the evolution of intra-oceanic arcs. Be-

cause the crustal structure in the northern part of the KPR appears to be complex due to the existence of the Daito Ridges to the west, we have located our seismic refraction profiles across the central part of the KPR. In this paper, we report the results of four profiles that were acquired in the fall of 2004.

2. Survey and Data Processing

The seismic survey comprised four seismic lines that were located across representative variations in seafloor topography - height and width of the bathymetric high and of the central KPR at 15–21°N (Fig. 1). All of the profiles cross the KPR almost perpendicularly, and their lengths are from north to south—180 km for KPr19, 175 km for KPr20, 370 km for SPr5, and 270 km for KPr26. The controlled seismic source provided by *M/V Tairikudana* was a tuned array of 36 airguns, with a total volume of 8040 inch³ (132 l). The airgun array was fired at a 50-m interval for the multi-channel (480 channels with 6,000-m-long streamer) seismic (MCS) reflection profiling. In the wide-angle seismic survey, however, the airgun array was fired approximately every 200 m for each line. We used 200 ocean bottom seismographs (OBS) in total with a 5-km receiver spacing. Each OBS instrument is equipped with a three-component 4.5-Hz geophone and a hydrophone. The outputs from the sensors were continuously recorded on hard disc at a sampling rate of 200 Hz with a resolution of 24 bits. Shot and OBS locations were provided by the ship's GPS navigation system, but each OBS was relocated using the direct water wave arrivals it recorded.

The OBS record sections are shown after 4- to 16-Hz bandpass filtering, predictive deconvolution (1st-zero cross-

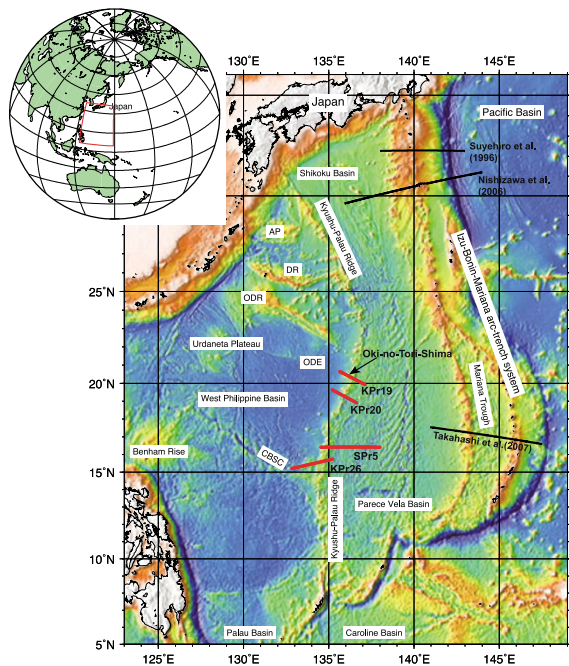


Fig. 1. Tectonic map of the Philippine Sea plate and location of the seismic profiles (red lines). Previous profiles across the Izu-Ogasawara (Bonin)-Mariana (IBM) Island arc are shown by black lines. AP: Amami Plateau, DR: Daito Ridge, ODR: Oki-Daito Ridge, ODE: Oki-Daito Escarpment, CBSC: Central Basin spreading center.

ing, operator length of 660 ms), and a local slant stack to enhance the signal-to-noise ratio. Travel times of the refraction and reflection signals were picked from these record sections. An initial velocity model was created with the upper sedimentary layer constrained by the MCS data. First arrivals were inverted for a two-dimensional (2-D) velocity model using the *tomo2d* tomographic inversion code of Korenaga *et al.* (2000). In the inversion, a horizontally homogeneous model for igneous crusts was initially assumed.

We then constructed the model from the shallower to deeper crust, increasing the offset limits of the input travel time data. In the velocity models derived on all four profiles, the horizontal grid spacing is 0.5 km, and the vertical grid spacing gradually increases with depth according to the relation $0.05 + [0.01 \times \text{depth (km)}]^{1/2}$ km.

The resolution of our velocity models was examined using checkerboard tests. We built a reference model by adding sinusoidal anomalies with a horizontal dimension of 10 km, a vertical dimension of 2.5 km, and a maximum amplitude of ± 0.3 km/s to the upper crust of our preferred final model. In the lower crust, cells were 30 km horizontally by 5 km vertically, with a maximum velocity perturbation of ± 0.5 km/s. The pattern of the checkerboard velocity anomalies is shown in Fig. 2. The pattern of the velocity anomalies is recovered well in the crust when the Moho depth is less than 15 km.

To model reflection arrivals and low-amplitude refraction signals at far offsets, we carried out forward modeling using a 2D raytracing algorithm (Fujie *et al.*, 2000; Kubota *et al.*, 2005). We used the tomographic model as an initial model of the ray tracing and then improved the raytracing model by try and error. If necessary, we used the raytracing model as an initial model of the inversion and confirmed the result. The final velocity models shown in Fig. 2 are the results of the forward modeling, and the checkerboard test was carried out for the final raytracing model. In a final step, 2-D synthetic seismograms were calculated by a finite difference method, E3D (Larsen and Schultz, 1995) and compared with the observed field data.

3. Results

Figure 2 shows the *P*-wave velocity model and the results of the checkerboard test for each profile. The root-mean-square (RMS) misfits between the observed and calculated first-arrival travel times for the final models are 60 ms for KPr19, 63 ms for KPr20, 71 ms for SP5, and 64 ms for

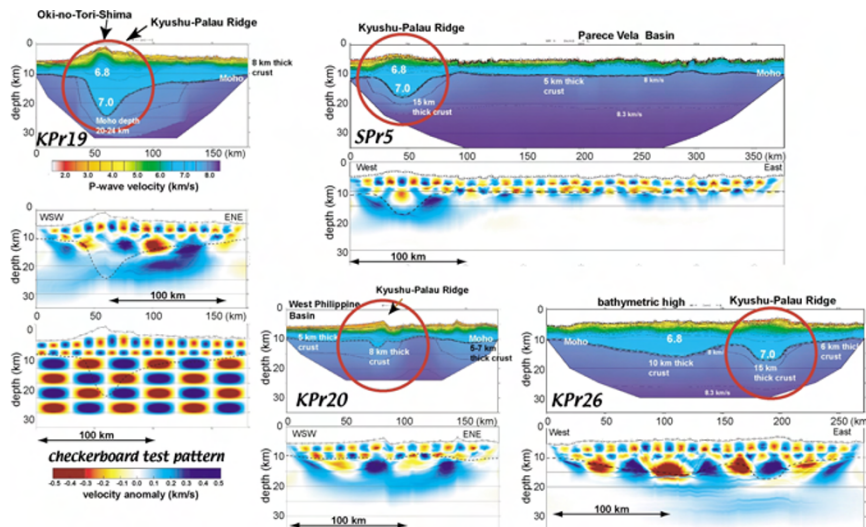


Fig. 2. *P*-wave velocity models derived from two-dimensional ray tracing and tomographic inversion. A red circle indicates the position of the Kyushu-Palau Ridge (KPR) for each profile. Iso-velocity contours with an interval of 0.25 km/s are shown for the region with a *P*-wave velocity larger than 3.5 km/s. The checkerboard test pattern for profile KPr19 is shown at bottom left. Same pattern is used for other profiles except for the bathymetry. The result of the checkerboard test is also shown below the each velocity model. Vertical exaggeration of models is 2.4.

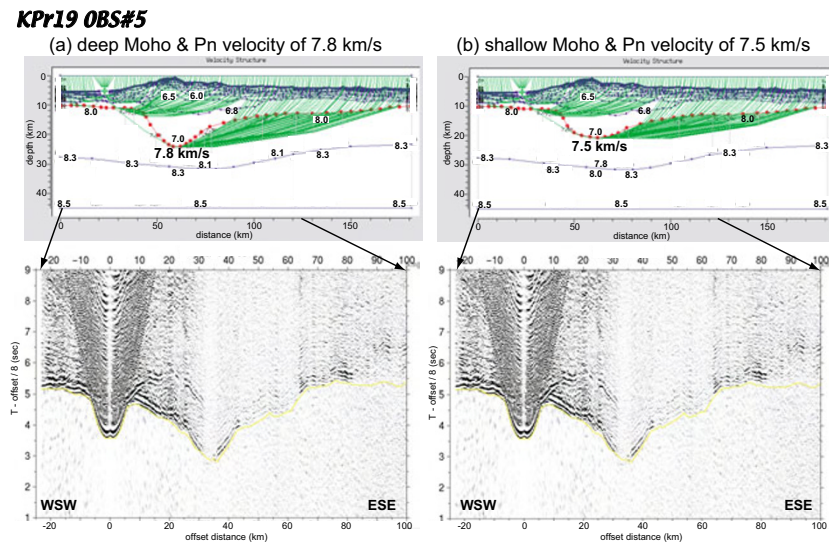


Fig. 3. Comparison of ray-diagram (top), observed record section, and calculated travel times shown by dots (bottom) for the different KPR models. The Moho depth beneath the KPR in the model (a) is deeper and the P_n velocity is faster than those in model (b). Both models can nicely explain the observed travel times.

KPr26. We describe the results of the individual seismic profiles from north to south.

The northernmost profile KPr19 crosses the shallowest and widest part of the KPR in the survey area (Fig. 1). Oki-no-Tori-Shima Island exists 50 km from the western end of the profile. The velocity model indicates a 20-km-thick crust near the island. However, the checkerboard test is poorly resolved in the lower crust. Due to the trade off between the crustal thickness of the KPR and P_n velocity beneath the ridge, it is difficult to determine the depth of the Moho with any precision. Figure 3 illustrates the ray diagram (top) and calculated travel times (yellow dots) on the observed record section (bottom) for two different models of the base of the KPR crust. The fit of the calculated to the observed travel times is similar in both these models, implying that the Moho could vary in depth between 20 km and 24 km with P_n values between 7.5 and 7.8 km/s. Other P_n velocity values do not fit well with the times of the observed P_n arrivals. PmP phases were observed in the limited areas where the Moho depths change at both sides of the ridge and the checkerboard pattern was recovered, but the PmP signals from the deepest part of the crust were not detected. Significant reflections indicating a middle/lower crust boundary in the KPR crust were not identified more than two continuous OBSs.

In terms of profile, KPr19, the crust of the West Philippine Basin to the west and the Parece Vela Basin (PVB) to the east, was divided into two layers on the basis of velocity and velocity gradient. We classified the upper crust as the layer with the P -wave velocity of 2.0–6.8 km/s and a relatively large velocity gradient of about 1 km/s per kilometer and the lower crust as the layer with velocities of 6.8–7.0 km/s and a smaller velocity gradient of 0.1 km/s per kilometer. Since several OBSs on the PVB recorded clear PmP arrivals, the Moho discontinuity was modeled as a velocity jump. The total crustal thickness was about 6–7 km. This velocity model is very similar to that of a normal oceanic crust.

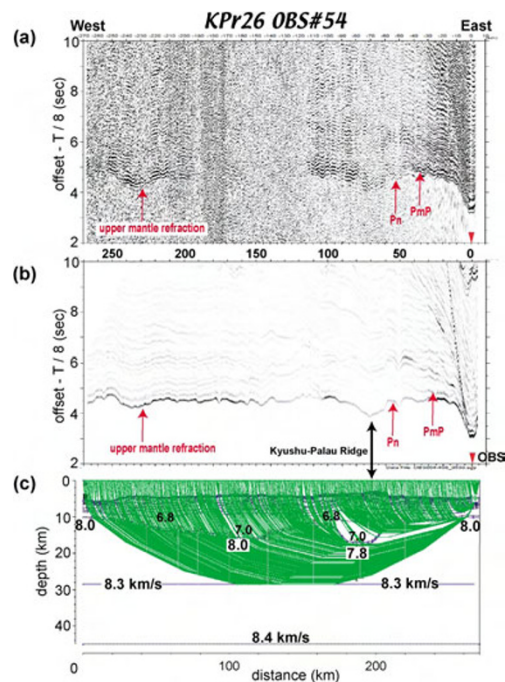


Fig. 4. (a) Vertical geophone record section for ocean bottom seismographs (OBS) 54, profile KPr26. A gain factor proportional to distance has been used to enhance the distant seismograms. The reduction velocity is 8 km/s. Small dots indicate calculated travel times. (b) Synthetic seismograms for OBS 54 calculated by the E3D model in Fig. 2. (c) Ray geometry through the upper mantle.

The water depth along profile KPr20 is the deepest among the four profiles. The crustal thickness, which is at most 8 km beneath the KPR, is also the least amongst the four profiles, but the crust beneath the KPR is still slightly thicker than the oceanic crust at either side. With the exception of the eastern end of the profile, the crust/mantle boundary is modeled as a transition rather than as a velocity jump since PmP arrivals were not identified.

The KPR lies at the western end of profile SPr5. We

inferred a velocity model with a crustal thickness of 15 km beneath the KPR and an uppermost mantle velocity of 7.8 km/s. The average crustal thickness of the PVB is only 5 km along this profile, and the crust is the thinnest 90 km from the western end of the profile, at the transition between the KPR and PVB where there is a depression in the seafloor.

On profile KPr26, the KPR is positioned towards the eastern end, and another bathymetric high exists in the west. The crustal thicknesses of both the KPR and the western bathymetric high are as great as 15 km, which is significantly thicker than normal oceanic crust. Large-amplitude arrivals at offsets greater than 200 km were observed on several OBSs on the both ends of the profile. An example of the record section at OBS 54 is shown in Fig. 4. The observed amplitudes indicating decay beyond 250 km can be explained by a change in the velocity gradient in the upper mantle. We have simulated these far-offset arrivals using a model in which the velocity gradient in the mantle decreases from 0.02 km/s per kilometer at depths of less than 28 km to 0.01 km/s per kilometer and depths greater than 28 km; the *P*-wave velocity at a depth of 28.5 km is 8.3 km/s.

4. Discussion

The results from the wide-angle seismic experiment show that the crust of the KPR at 15–21°N can be represented as an upper crust with *P*-wave velocities <6.8 km/s and a large velocity gradient over a lower crust of 6.8–7.0 km/s and small velocity gradient. The maximum crustal thickness beneath the KPR ranges from 8 to approximately 20 km in the survey area. Seismic velocities characteristic of normal oceanic crust (e.g. White *et al.*, 1992) are inferred on both sides of the KPR - that is, the West Philippine Basin to the west and the Parece Vela Basin to the east. Therefore, the crust of the KPR is significantly thicker than the oceanic crust. The thickest crust along the ridge occurs close to the intersection of the KPR with Oki-no-Tori-Shima Island. The crustal thickness of about 20 km is similar to that of the conjugate rifted counterpart of the IBM arc (Suyehiro *et al.*, 1996; Nishizawa *et al.*, 2006; Takahashi *et al.*, 2007).

The thicker crust beneath the KPR is mainly due to the presence of a thicker lower crustal layer. The thick (>5 km) middle crusts with a *P*-wave velocity of approximately 6 km/s and the velocity discontinuity at the mid/lower crust boundary, both of which characterize the IBM arc crust, do not exist in our KPR profiles. This result may indicate that the deeper water depths along the central KPR indicate the presence of immature island arc crust compared with the northern KPR where a 6 km/s-layer has been reported (Shinohara *et al.*, 1999). This thinner KPR middle crust may be due to its rifting from the edge of the Mariana arc where the arc crust was not particularly thick.

P-wave velocities of less than 8 km/s are required in the uppermost mantle beneath the KPR to explain the observed record sections, although they are difficult to determine accurately because the width of the KPR is not particularly large. The lower *P_n* velocity is similar to that of the IBM arc crust (Suyehiro *et al.*, 1996; Nishizawa *et al.*, 2006; Takahashi *et al.*, 2007). Higher velocities of about 7.2 km/s inferred near the base of the IBM arc crust cannot be clearly identified beneath the central KPR due to a lower

ray density in the lower crust.

Large-amplitude signals clearly recorded at offsets over 200 km at the profiles KPr26 were also observed at several OBSs along SP5 in the Parece Vela Basin. These signals could be explained by a change in velocity gradient from 0.02 km/s per kilometer to less than 0.01 km/s per kilometer at the depths of 24–29 km in the upper mantle. Such changes in the velocity gradient in the uppermost mantle of the Philippine Sea plate may be related to an earthquake cluster at depths of 20 km in the uppermost mantle detected in the 2004 off the Kii Peninsula earthquake (*M*=7.4) (Sakai *et al.*, 2006).

Acknowledgments. The authors gratefully acknowledge the members of Continental Shelf Surveys Office, HODJ, for the management of the seismic surveys. The comments and suggestions from Drs. S. Kodaira, N. Takahashi and Y. Kaneda, JAMSTEC were greatly appreciated. Numerous comments of the reviewers, Drs. A. J. Calvert and K. Mochizuki helped considerably to improvement in the manuscript. Data acquisition and processing were carried out by Japan Continental Shelf Survey Cooperation. Most of the figures in this paper were made using the GMT graphic package of Wessel and Smith (1998).

References

- Fujie, G., J. Kasahara, T. Sato, and K. Mochizuki, Traveltime and raypath computation: A new method in a heterogeneous medium, *J. Soc. Expl. Geophys. Jpn.*, **53**, 1–11, 2000.
- Kodaira, S., T. Sato, N. Takahashi, S. Miura, and Y. Kaneda, Structural variation from mature to juvenile arc crust along the Izu Bonin arc, *Eos Trans. AGU*, **87**(52), Fall Meet. Suppl., Abstract, V41B-1711, 2006.
- Korenaga, J., W. S. Holbrook, G. M. Kent, P. B. Kelemen, R. S. Detrick, H.-C. Larsen, J. R. Hopper, and T. Dahl-Jensen, Crustal structure of the southeast Greenland margin from joint refraction and reflection seismic tomography, *J. Geophys. Res.*, **105**, 21591–21614, 10.1029/2000JB900188, 2000.
- Kubota, R., E. Nishiyama, K. Murase, and J. Kasahara, Fast computation algorithm of ray-paths and their travel times including later arrivals for a multi-layered earth model, *Eos Trans. AGU*, **86**(52), Fall Meet. Suppl., Abstract, S41A-0966, 2005.
- Larsen, S. C. and C. A. Schultz, ELAS3D: 2D/3D elastic finite-difference wave propagation code, LLNL internal report, 18 p., 1995.
- Nishizawa, A., K. Kaneda, A. Nakanishi, N. Takahashi, and S. Kodaira, Crustal structure of the ocean-island arc transition at the mid Izu-Ogasawara (Bonin) arc margin, *Earth Planets Space*, **58**, e33–e36, 2006.
- Okino, Y., Ohara Y., S. Kasuga, and Y. Kato, The Philippine Sea: New survey results reveal the structure and the history of the marginal basins, *Geophys. Res. Lett.*, **26**, 2287–2290, 1999.
- Sakai, S., T. Yamada, M. Shinohara, H. Hagiwara, T. Kanazawa, K. Obana, S. Kodaira, and Y. Kaneda, Urgent aftershock observation of the 2004 off the Kii Peninsula earthquake using ocean bottom seismometers, *Earth Planets Space*, **57**, 363–368, 2005.
- Shinohara, M., N. Takahashi, K. Li, K. Suyehiro, and A. Taira, Crustal structure of the northern Izu-Bonin arc and Kyushu-Palau Ridge by controlled-source seismology, *Monthly Earth*, **23**, 67–78, 1999 (in Japanese).
- Suyehiro, K. *et al.*, Continental crust, crustal underplating, and low-*Q* upper mantle beneath an oceanic island arc, *Science*, **272**, 390–392, 1996.
- Takahashi, N., S. Kodaira, S. L. Klemperer, Y. Tatsumi, Y. Kaneda, and K. Suyehiro, Crustal structure and evolution of the Mariana intra-oceanic island arc, *Geology*, **7**, 383–394, 2007.
- Wessel, P. and W. H. F. Smith, New, improved version of the Generic MappingTools released, *EOS Trans. AGU*, **79**, 579, 1998.
- White, R. S., D. McKenzie, and R. K. O’Nions, Oceanic crustal thickness from seismic measurements and rare earth element inversions, *J. Geophys. Res.*, **97**, 19683–19715, 1992.